NAME III Document
MD13/9(version 1)
01/06/05

Investigating the ability of NAME III to model a uniform field of concentration

Andrew Jones and David Thomson, Atmospheric Dispersion Group

1 Introduction

A desirable quality for any dispersion model would be its ability to maintain a uniform concentration of a tracer throughout the model domain when it is run in the presence of a steady uniform tracer concentration maintained around the edges of that domain. Such a characteristic is dependent both on mass conservation in the flow field of the dispersion model and on a consistent representation of the turbulent mixing in the model. The former is primarily governed by the mass-conserving abilities of the driving meteorological model (although the way in which the flow field is set up in the dispersion model to use the meteorological input is also important). The response of the dispersion model to orography is often a key issue here. Meanwhile, the latter is significant in the sense that any inconsistencies in the specification of turbulence levels can create regions where mass tends to converge or diverge (essentially this happens whenever particles find it 'easier' to enter a region than to leave that region, or vice-versa, and so particles either tend to accumulate or tend to be absent). Here the behaviour of the dispersion adjacent to the surface and near to the top of the boundary layer is an issue where difficulties are perhaps most likely to occur.

The capacity of a model to maintain a uniform field over periods of several days has implications for many applications but, in particular, maintenance of a uniform field has special value for chemistry applications. This is partly because of the need to adequately model the long-range transport of background fields (such as the hydroxyl radical and hydrogen peroxide). The relatively long time scales involved for some chemistry processes is another important issue (e.g. in the modelling of species such as ozone). In these cases, relatively small deviations in concentrations that might develop from weaknesses in the mass conservation of the dispersion model could potentially be amplified during this time by non-linearity in the chemical reactions set. In this way, poor mass conservation by the dispersion model could, after running the model over several days, allow large errors to develop in the concentration fields and seriously degrade the accuracy of model predictions. A good performance in our uniform field test should therefore increase our confidence that model results are not being adversely affected by the dispersion aspects of the simulation.

The ability to maintain uniform concentration fields in NAME III (version 2.0) is investigated in this report. Also our focus here will be on the use of NWP meteorological data within NAME III. However, as an aside, it might be useful to briefly discuss the use of single-site met data in NAME III from a uniform-field viewpoint. When single-site data is used (e.g. observations at a particular station), that meteorology is assumed to be horizontally homogeneous across the extent of its meteorological domain. Over large domains, single-site meteorological input does not work well (as might be expected) since there is the problem of divergence in the flow field with changing latitude. With smaller domains, the curvature of the earth is not as significant and better results should be obtained. However it is worthwhile to point out the following scenario where difficulties can occur. When there is no velocity memory in the random walk scheme but the 'exponential' damping fix-up is used to emulate the near-source dispersion regime then a difference in turbulence levels will exist between particles of different ages. Old particles within the domain have higher levels of turbulence than younger particles recently created in one of the sources around the edge. Consequently, particles tend to find it easier to escape the domain than they do to enter the domain. This is unlikely to cause problems in general, because the transport is dominated by the mean flow, but it can give difficulties in idealised cases (e.g. where the mean flow is aligned with one of the domain boundaries).

2 The modelling methodology

The principles underlying our uniform field test are now discussed, including the main features of the NAME III model set up used in the study. The basic idea is that the primary model domain (i.e. the region in which we wish to maintain a uniform concentration of tracer) is surrounded by a halo region where the concentration is artificially forced to a prescribed value. This background concentration is realised in the outer halo region by prescribing a uniform (cuboid) source term adjacent to each face of the inner domain (i.e. along the northern, southern, eastern and western edges as well as the upper lid), see Figure 1. In this way, at the same time as the tracer material is being advected out of the domain at some locations, so there will be other locations where tracer is being imported into the domain with the desired mass flux. For a dispersion model exhibiting perfect mass conservation, the local concentration of tracer should remain a function of pressure only (strictly speaking, tracer concentration will be a function of the atmospheric density rather than purely atmospheric pressure, but the source terms are only defined relative to pressure in these runs). Of course, we should expect some statistical noise in the instantaneous concentration field (related to the number of particles being tracked) but this should be reduced both with spatial and temporal averaging. Any systematic problems with the mass conservation in the model should become apparent in this type of run.

We consider a rectangular domain in the standard latitude-longitude coordinate system (such that its edges are aligned north-south and east-west). Two vertical coordinate systems are required: a pressure-level coordinate (pressure in Pa) for defining the modelling domain and sources, and height above ground level for calculating output concentrations. All sources are defined as cuboids with sharp edges (i.e. the 'Top Hat' flag is set to true). The horizontal extent is specified in latitude-longitude coordinates, and the vertical extent in pressure coordinates (so that the release is uniform in pressure rather than height). The 'Uniform Area?' and 'No Reflect?' flags are used here. The former ensures that particles are released uniformly by area (rather than uniformly in the coordinates x and y). This distinction is significant when using large area sources defined in a latitude-longitude system due to the curvature of the earth. The latter causes particles released beneath the ground to be killed off (rather than being reflected), and

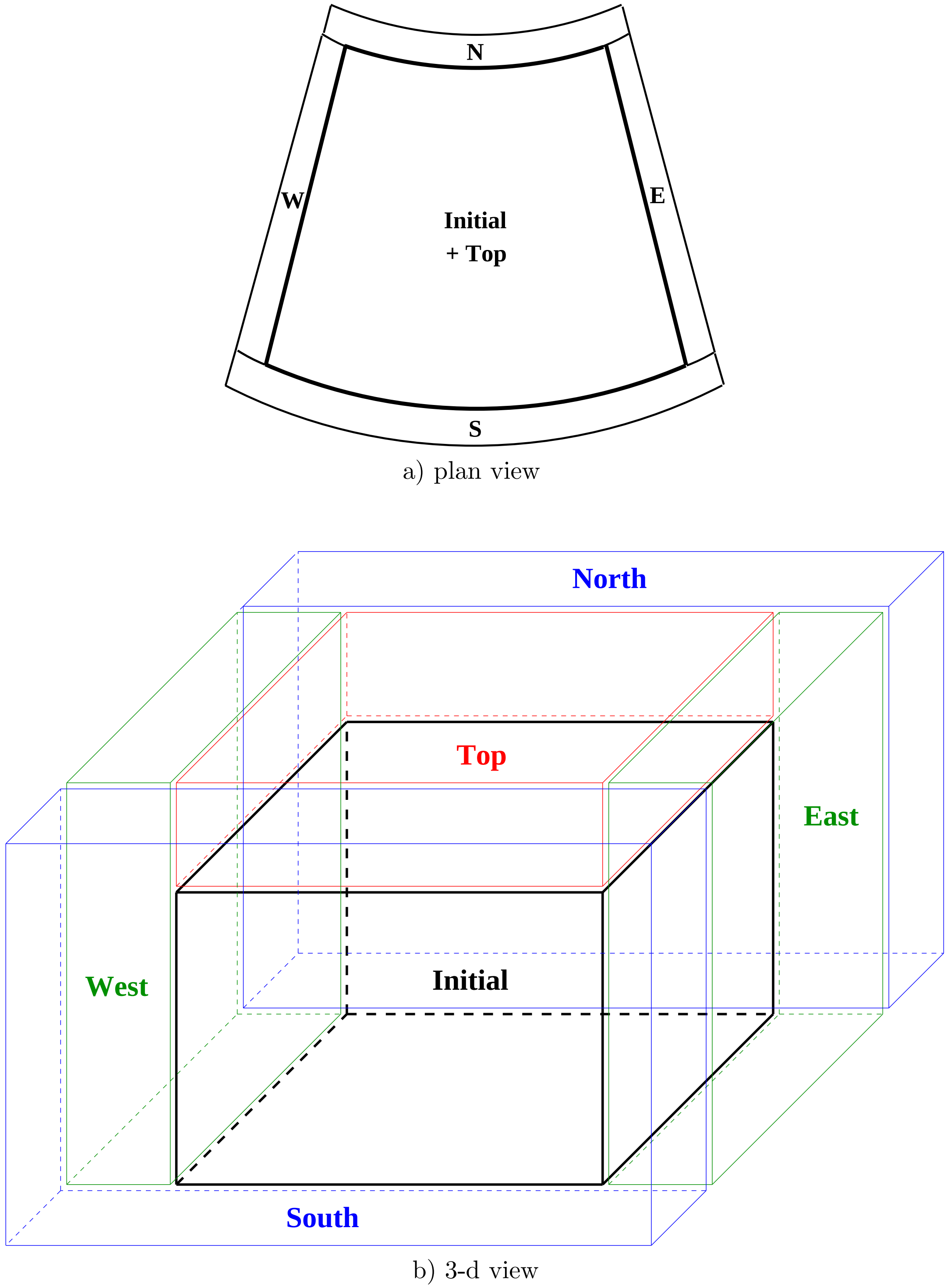

Figure 1: Configuration of sources for our uniform field tests. The initial source term provides a uniform concentration of tracer throughout the primary model domain at the start of the run. Edge sources adjacent to the top, northern, southern, eastern and western faces ensure that any tracer advected into the domain during the run has the correct concentration.

is required to ensure a uniform release in the vertical coordinate. Calculation of the detailed source parameters (volumes, source strengths, etc.) is included in the next section.

Three domains are defined: an 'inner domain' (the primary model domain), a 'halo domain' containing the edge sources, and a fully unbounded domain. The inner domain is spatially bounded but there is no limit on the travel time (lifetime) of particles in this domain; the halo region is spatially unbounded but the travel time of particles is restricted to 7.5 minutes (see below); and the unbounded domain is completely unbounded (both in terms of space and travel time). In addition, two NWP flow module instances are prescribed. Both of these are based on the same regional met data but have different underlying domains: one uses the inner domain (i.e. is space limited) and allows us to follow particles in the usual way within the primary modelling domain, and the other uses the halo domain (i.e. is travel-time limited) and enables the edge sources to be controlled in the correct manner.

The dispersion is modelled using particles in this study (we do not consider puffs at all here, primarily because puffs are intended for use at short ranges while this study is interested in the long-range dispersion behaviour). The cheap random-walk scheme is applied (i.e. homogeneous turbulence with no velocity memory) using a 15-minute synchronisation interval (main advection time step). The effects of both turbulence and meander are included here, although the effect of deep convection is not considered in our runs. The material is modelled as an inert tracer, i.e. there are no decay processes and no dry nor wet deposition. Also chemistry is inactive.

3 Results for UM 5 met data

The ability of NAME III to maintain a uniform concentration of tracer is tested using NWP meteorological data from UM 5 (the 'new dynamics' version of the Met Office Unified Model). Here we use 'regional' met data (i.e. a cut-down subset of the global model output) which has a spatial resolution of $5/6^o$ (Δ Long) by $5/9^o$ (Δ Lat). A minimum boundary-layer depth of 50 m and a maximum of 4 km is imposed. The model orography of the UM 5 global model is shown in Figure 2 (although note that the topography is plotted here at a 1^o x 1^o resolution). In particular, note the areas with high topography (especially the Alps, northern Spain and Norway).

The test case using UM 5 met data considers the period starting at 00 UTC on 01/01/2003 and finishing at 00 UTC on 11/01/2003. This gives a run duration of 10 days (240 hours). Analysis charts for this period are included in Appendix A. With the exception of the final run reported below, the primary model domain (the 'inner domain') used in these tests has the horizontal extent (15^oW – 20^oE, 43^oN – 65^oN), and extends vertically to a pressure level of 400 hPa. The final model run adopts a somewhat smaller horizontal domain, covering the region (8^oW – 4^oE, 47^oN – 57^oN), and again extends vertically to a pressure level of 400 hPa. This allows an approximate four-fold increase in the number of particles per grid box while following roughly the same total number of particles.

The source terms are calculated (see below for details) to produce a target background concentration of approximately 24 mg m^{-3} next to the surface and a corresponding vertically-integrated concentration of about 160 g m^{-2} (except for the final

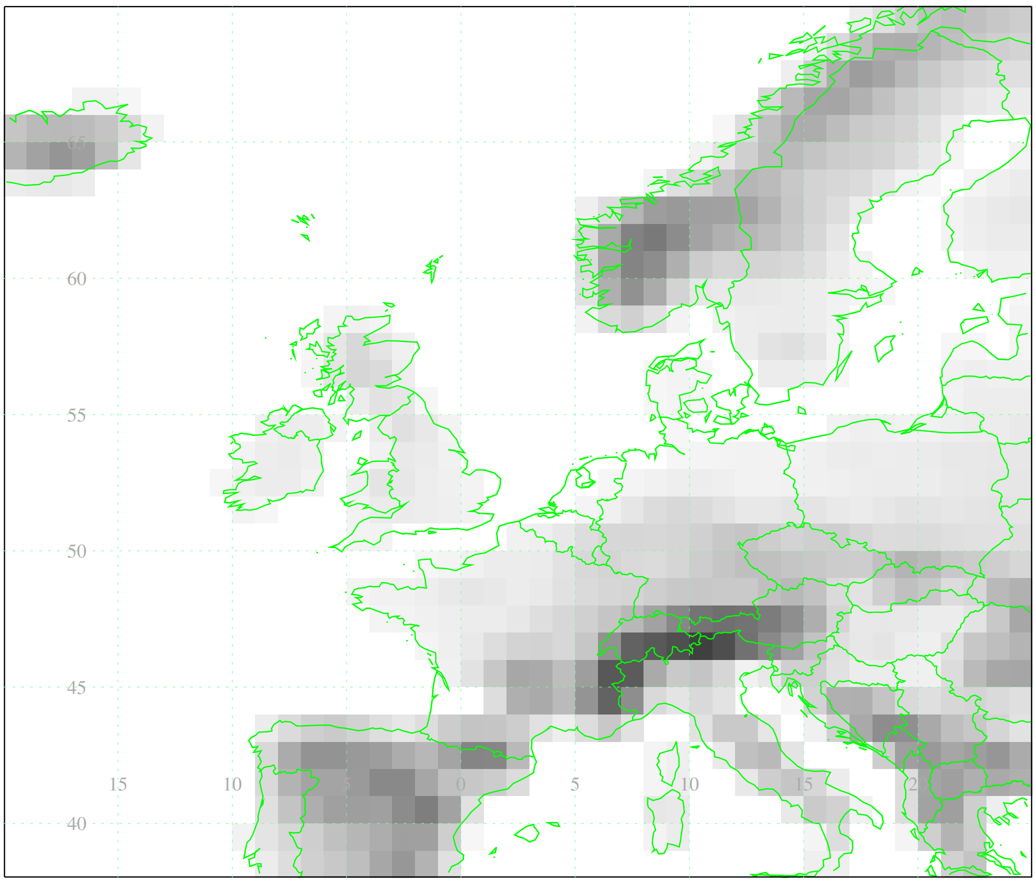

Figure 2: Model orography of the UM 5 global model degraded to the 1^o x 1^o resolution of the NAME III output grid used in our uniform field tests. Darker shades indicate higher orography.

model run where the target surface-level concentration is 40 mg m^{-3}).[1] These target concentrations were chosen in a largely arbitrary way, and for future consideration, it is probably more sensible to aim for a background concentration of, say, 1 g m^{-3} at standard surface pressure. Note that we control the number of particles that are released from the sources (and therefore, ultimately, the number of particles defined in the model run) using the 'Particle Mass' parameter (again, see below for details). This parameter specifies the mass carried by any single particle and is set to ensure a global particle number of approximately 2.5 million in each of these runs.

A variety of quantities are requested as output, both as fields and as time series at specific locations. Field output is calculated on a 1^o x 1^o horizontal grid, and includes air concentrations over the two layers 0 – 100 m and 0 – 500 m, boundary-layer average concentration, and vertically-integrated concentration. These quantities are calculated as instantaneous values, hourly-average values (based on four contributions during each hour – consistent with the 15-minute synchronisation interval) and 5-day averages (based on 120 instantaneous hourly values over that period). Time-series output is calculated using a 1^o x 1^o box around each location, and consists of hourly-average values of the 0 – 100 m air concentration (again constructed using four contributions in each hour).

In plotting the field output, we choose contours at the following ratios of the nominal concentration (or concentration integral): 0.000, 0.125, 0.375, 0.625, 0.875, 1.125, 1.375, 1.625, 1.875, 2.000 and 4.000. In other words, the central (light orange) band here represents a range of $\pm 12.5\%$ around the nominal value, with successive 25% changes over adjacent bands. The output grid for the concentration fields extends 5^o in each direction beyond the primary model domain. This extended output grid is useful for examining the behaviour of the concentration on the peripheries of the main domain and in the edge sources, although it should be stressed that a uniform concentration is only expected to be present in the primary domain here. In particular, the manner in which the edge sources operate gives a variable concentration in these source regions over each 15-minute interval between particle synchronisations (since aged particles are only killed off in the halo domain at the end of the synchronisation step). The source terms are constructed such that the mean number of particles averaged over each time step is correct, but the output is calculated at the end of the time steps when the concentration is over-represented. Hence the source regions indicate an apparently greater concentration than in the primary domain. Note that the impact of the fluctuating source terms on the uniform field test itself is likely to be small (at least when we are considering synoptic-scale domain sizes), but for the future it is worth considering the ability to kill off particles immediately their lifetime expires and so avoid these fluctuating sources.

Before we present the results of these simulations, it might be useful here to first say a few words about what should be expected. In particular, we do not expect a 'uniform' field (at least, when expressed in terms of mass concentration which is the quantity calculated here) because mass concentration falls off with height as the atmospheric density decreases. As a consequence, the model orography will have an influence on the values. For air concentration averaged over a layer (0 – 100 m, 0 – 500 m or boundary layer), a uniform field is expected to be proportional to the air density of that layer. For

[1] It is not possible to give specific values here since we are considering *mass concentrations* (i.e. mass per unit volume), so that even a well-mixed pollutant will exhibit a decreasing concentration with height as the atmospheric density decreases.

vertically-integrated air concentration, the model orography provides the lower height bound on the integration, and so lower values are again expected over orography.

Figure 3 shows the (instantaneous) value of the atmospheric density at 10 m above ground level at the end of the first day. Note that variations in the density are relatively small and so a non-linear scale is used here to emphasise them in the plot. Air density generally increases as the air becomes colder towards the north. The impact of orography is also evident here, with lower air density over higher ground (c.f. Figure 2). The lower air density is most notable over the Alps and northern Spain, but Norway, Italy and the Balkans are also clearly distinguishable here.

3.1 Calculation of the source terms

As briefly mentioned above, the source terms need to be calculated such that they lead to the desired background concentration in the primary model domain. This calculation essentially involves calculating the volume of each source and then the mass that must be released per second to achieve the target concentration.

We first consider the initialisation of a uniform tracer concentration throughout the primary model domain at the start of the model run. This initial source term takes the form of an instantaneous release occurring at 7.5 minutes into the run (the centre of the first synchronisation time step). The mass to be released at this time $m_{initial}$ is calculated by multiplying the total mass of tracer in a vertical column of unit area by the area of the primary domain. The mass per unit area in a vertical column extending over a pressure difference Δp is given by $(\Delta p/g) \times \rho/\rho_a$, where ρ and ρ_a are the tracer density and atmospheric density, respectively, and g is the gravitational acceleration. Meanwhile, the horizontal area of a region with longitude extent $\Delta\lambda$ and latitude extent $\Delta\phi$ is given by $\iint r_E\, d\lambda\, r_E cos\phi\, d\phi = r_E^2 \Delta\lambda\Delta(sin\phi)$, where $r_E = 6{,}371{,}229$ m is the Earth radius, and λ and ϕ denote longitude and latitude, respectively.

The easiest method of calculating release rates for the edge sources is to determine their relative volumes with respect to the primary domain and then to scale the mass in the appropriate way. Note that to obtain the same tracer concentration in the halo region as exists in the main domain, we need to release this equivalent quantity of mass over the synchronisation interval (rather than the instantaneous release considered above). Here a synchronisation interval of 900 seconds is used. Hence the mass release rate for an edge source (in g s^{-1}) is obtained as $\Delta V \times m_{initial}/900$, where ΔV denotes the ratio of the volume of the edge source to that of the initial source. This construction also accounts for the travel-time limit of 7.5 minutes imposed on particles in the halo region (see earlier). This restriction on the travel time is needed to give an average travel time of 15 minutes in this domain (the difference here is because particles are not killed off until the end of each synchronisation interval!). If a particle has not entered the primary domain by this time, then it will expire. Hence a quasi-uniform concentration will be maintained in the edge sources over the duration of the model run.

The dimensions of the edge sources and the calculation of their mass release rates are given in Table 1 (for the large primary domain) and Table 2 (for the small primary domain). Here (λ_0, ϕ_0, p_0) denotes the centre point of a source, and $(\Delta\lambda, \Delta\phi, \Delta p)$ gives its spatial extent in each dimension. Finally, the 'Particle Mass' parameter is set to give approximately 2.5 million particles during a run: Particle Mass $= 5.0 \times 10^8$ g when using the large domain, and Particle Mass $= 1.75 \times 10^8$ g when using the small domain.

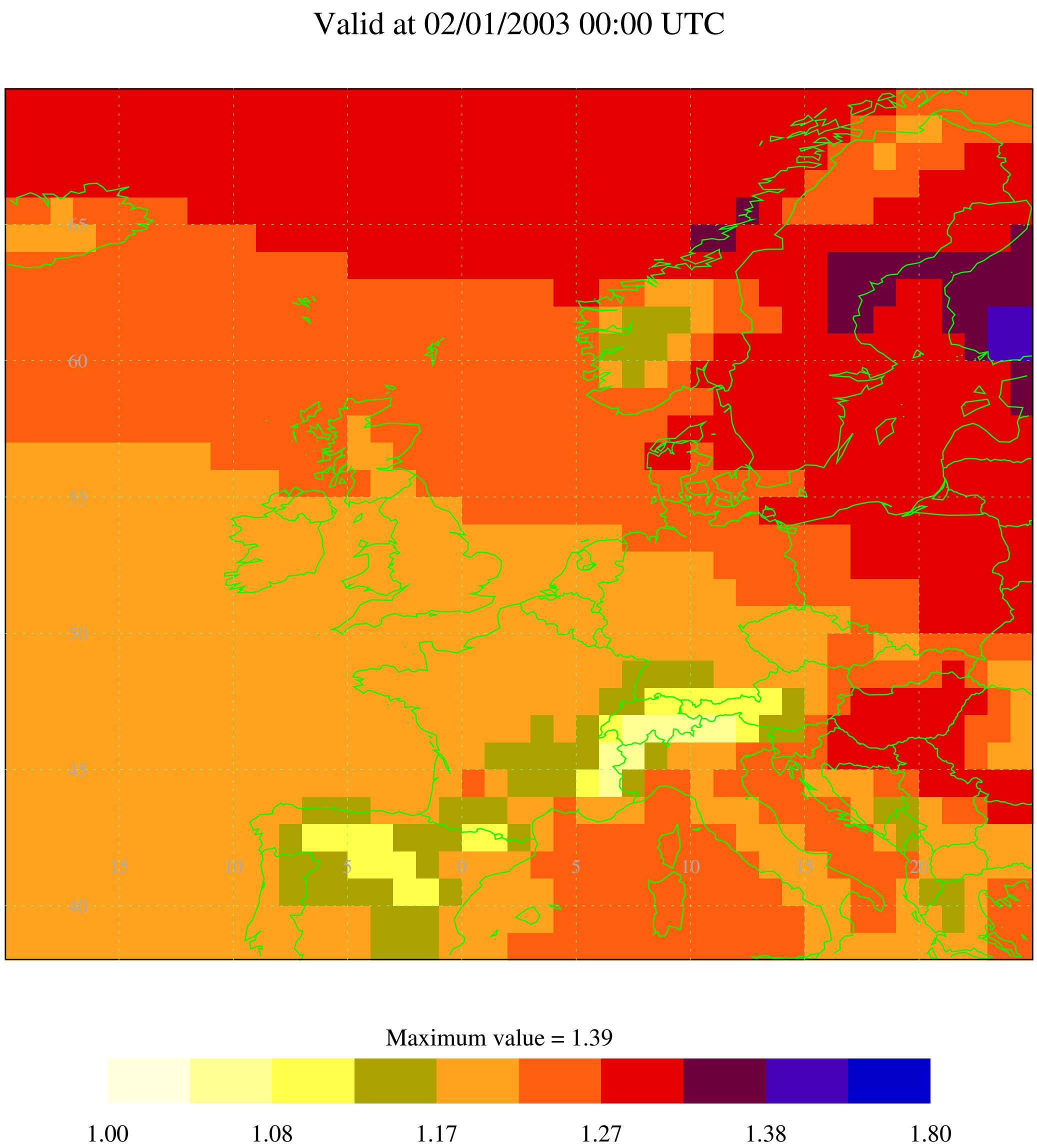

Figure 3: Air density at 10 m above ground level for 00 UTC on 02/01/2003 (i.e. end of the first day). Units are kg m^{-3}. Note the lower air density over topography, especially evident here over the Alps, northern Spain and Norway.

Source	λ_0	ϕ_0	p_0	$\Delta\lambda$	$\Delta\phi$	Δp	Release rate
	^{o}	^{o}	hPa	^{o}	^{o}	hPa	
Initial	2.5	54.0	800	35.0	22.0	800	9.0×10^{14} g
Top	2.5	54.0	350	35.0	22.0	100	0.125×10^{12} g/s
West	-16.0	54.0	750	2.0	22.0	900	0.0642856×10^{12} g/s
East	21.0	54.0	750	2.0	22.0	900	0.0642856×10^{12} g/s
South	2.5	42.0	750	39.0	2.0	900	$0.14496405 \times 10^{12}$ g/s
North	2.5	66.0	750	39.0	2.0	900	$0.079341482 \times 10^{12}$ g/s

(a) source dimensions and mass release rates

Source Ratio	$dA/d\lambda$	$\Delta\lambda$	Δp	ΔV
Top/Initial	1.0	1.0	0.125	0.125
West/Initial	1.0	0.0571428	1.125	0.0642856
East/Initial	1.0	0.0571428	1.125	0.0642856
South/Initial	0.11564084	1.1142857	1.125	0.14496405
North/Initial	0.06329235	1.1142857	1.125	0.079341482

(b) calculation of the volume ratios

Table 1: Source terms for use with the large primary domain. Here $\Delta(sin\phi)_{North} = 0.014197$, $\Delta(sin\phi)_{South} = 0.0259393$ and $\Delta(sin\phi)_{Initial} = 0.2243094$.

Source	λ_0	ϕ_0	p_0	$\Delta\lambda$	$\Delta\phi$	Δp	Release rate
	^{o}	^{o}	hPa	^{o}	^{o}	hPa	
Initial	-2.0	52.0	800	12.0	10.0	800	2.43×10^{14} g
Top	-2.0	52.0	350	12.0	10.0	100	0.03375×10^{12} g/s
West	-9.0	52.0	750	2.0	10.0	900	0.050625×10^{12} g/s
East	5.0	52.0	750	2.0	10.0	900	0.050625×10^{12} g/s
South	-2.0	46.0	750	16.0	2.0	900	$0.09150479 \times 10^{12}$ g/s
North	-2.0	58.0	750	16.0	2.0	900	$0.06980428 \times 10^{12}$ g/s

(a) source dimensions and mass release rates

Source Ratio	$dA/d\lambda$	$\Delta\lambda$	Δp	ΔV
Top/Initial	1.0	1.0	0.125	0.125
West/Initial	1.0	0.1666666	1.125	0.1875
East/Initial	1.0	0.1666666	1.125	0.1875
South/Initial	0.22593775	1.3333333	1.125	0.33890662
North/Initial	0.17235624	1.3333333	1.125	0.25853436

(b) calculation of the volume ratios

Table 2: Source terms for use with the small primary domain. Here $\Delta(sin\phi)_{North} = 0.0184967$, $\Delta(sin\phi)_{South} = 0.0242469$ and $\Delta(sin\phi)_{Initial} = 0.1073168$.

3.2 Spin-up behaviour of the model

An initial run was performed to investigate the 'spin-up' behaviour of the model when starting with zero concentration across the primary model domain. That is, to study whether NAME III could build up a uniform field of tracer from material being imported from the boundaries, and the length of time likely to be needed for this process. This spin-up run uses the large primary domain (15^oW – 20^oE, 43^oN – 65^oN).

Figure 4 shows the instantaneous value of the vertical integral of the air concentration at the end of each of the first six days of the model run. Note that later frames (not shown here) are generally similar to the final one shown (i.e. at the end of day six) although the region of low concentration on the northern side of the Alps (France and Germany) becomes less extensive by the end of the run. These plots demonstrate that there are no obvious problems evident with the spin-up of a uniform concentration field. There is rapid advection of tracer across the southern half of the model domain during the first couple of days of the run (associated with a strong WSW'ly flow at this time). Across the more northern parts of the domain, the flow is generally weaker (initially cyclonic but later becoming anticyclonic over the UK) and so the tracer requires more time to penetrate into this region. Over the entire domain, the time scale for the spin-up process is around five or six days in this particular instance. Of course, in general, the spin-up time is expected to be a function of the domain size and the synoptic meterorological situation. It can also be seen in these plots that the vertically-integrated concentrations are generally lower over high orography (Alps and Norway) as is to be expected from the earlier discussion.

We choose to perform our main modelling runs without an initial spin-up of the tracer by instead initializing a uniform tracer concentration throughout the model domain. This is achieved by having an instantaneous release during the first time step and offers the benefit of shorter (and therefore computationally cheaper) runs.

3.3 Long-term average concentrations

Let us first inspect long-term average concentrations. Here we consider mean values calculated over the five-day period at the end of the simulation (that is, over the interval 01 UTC, 06/01/2003 – 00 UTC, 11/01/2003). The reason for studying the long-term averages is that any systematic problems in the ability of NAME III to maintain a uniform field should be apparent. Figure 5 shows the vertically-integrated concentration field. It is clear that the uniform field has been maintained well over this period (at least, on average through this period). The vertical integral lies within $\pm 12.5\%$ of its nominal value over most of the primary domain, except for the lower values evident over high orography (which are to be expected). Figure 6 plots the air concentration calculated over two layers (a) 0 – 100 m and (b) 0 – 500 m. In both cases, the concentration remains uniform across most of the domain, although the results are somewhat noisier than those for the vertical integral because we are now averaging over a shallower depth of atmosphere and should therefore expect a greater amount of statistical noise. This is especially evident in (a) where the air concentration is calculated over a 100 m layer. Once again, we generally observe lower air concentrations over the Alps. There is also some evidence here of elevated concentrations to the lee of the high ground of Norway (and to a lesser extent over south-western parts of France and the east coast of the UK).

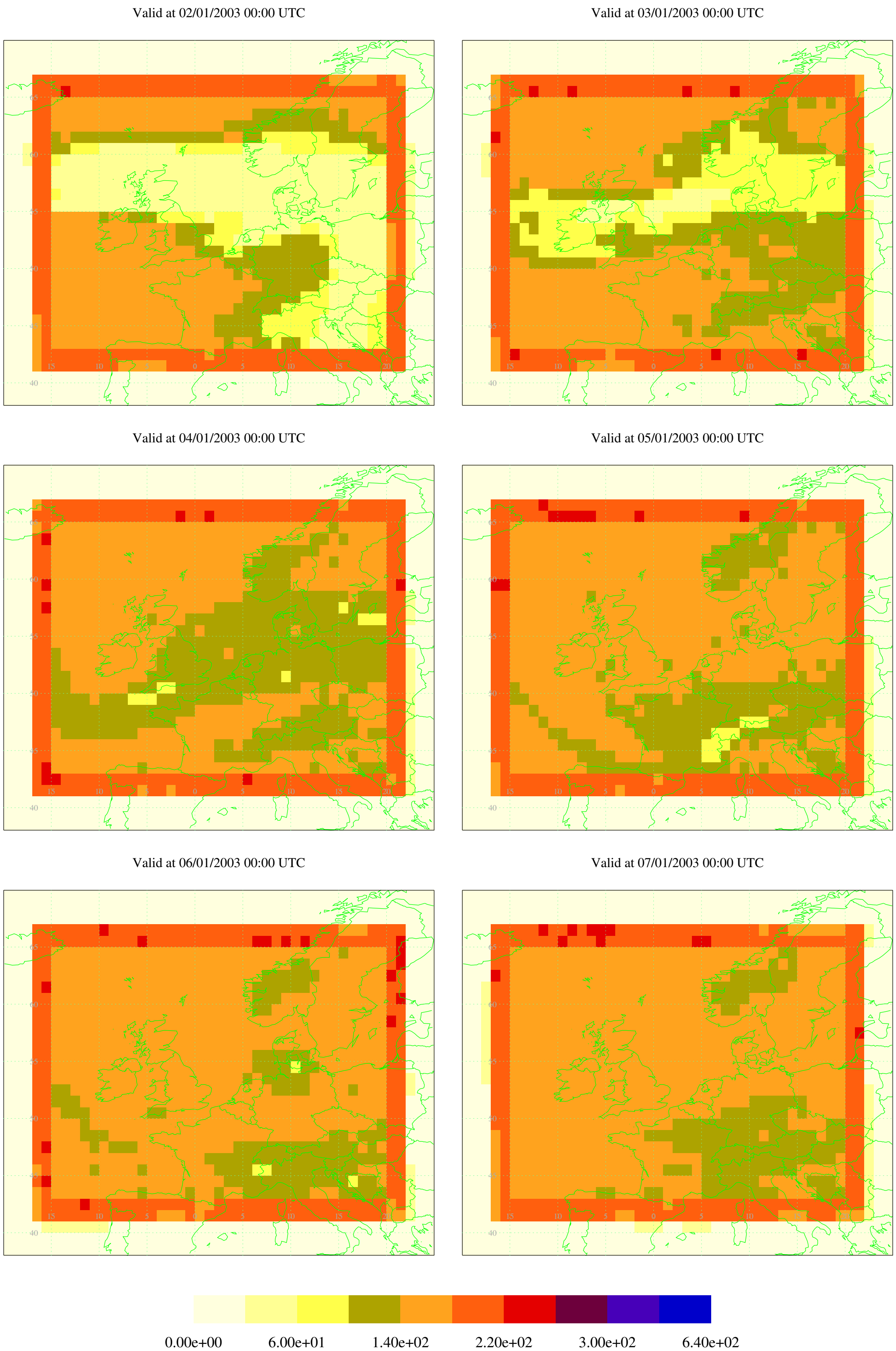

Figure 4: Vertically-integrated concentration at the end of each of the first six days illustrating the 'spin-up' of the model run. Units are g m^{-2}.

In summary, NAME III appears to be very capable of maintaining a uniform field (at least in a time-averaged sense) over the duration of the model run.

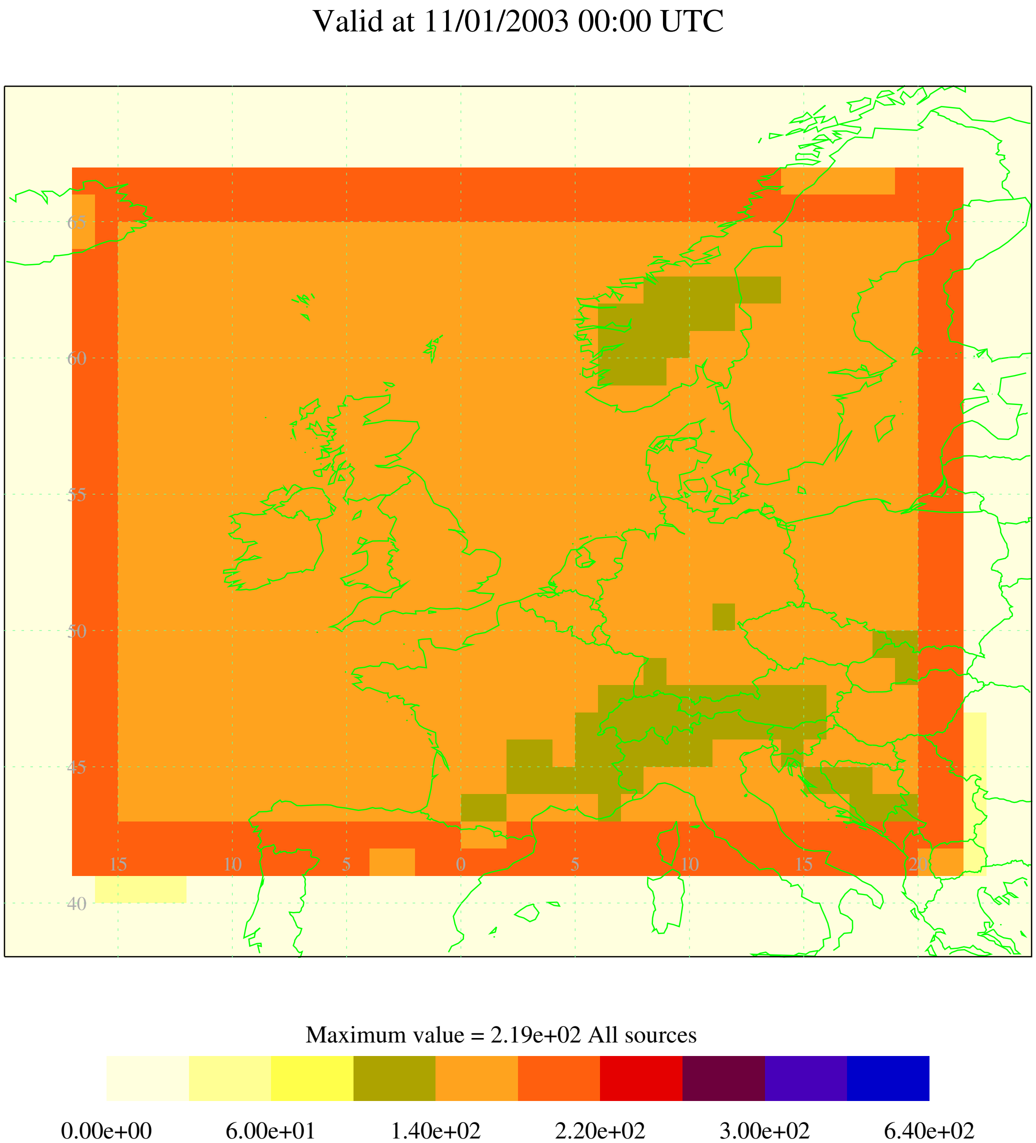

Figure 5: Vertically-integrated concentration calculated as a 5-day average over the period 01 UTC, 06/01/2003 – 00 UTC, 11/01/2003. Units are g m^{-2}.

3.4 Short-term features

We have seen that NAME III is able to model a uniform field of tracer as a long-term average, but it is also desirable to maintain uniform concentration over shorter time scales. Of course, as the averaging period becomes shorter so the level of statistical noise will increase. Hence we should not expect the concentration fields to be as smooth

(a)

(b)

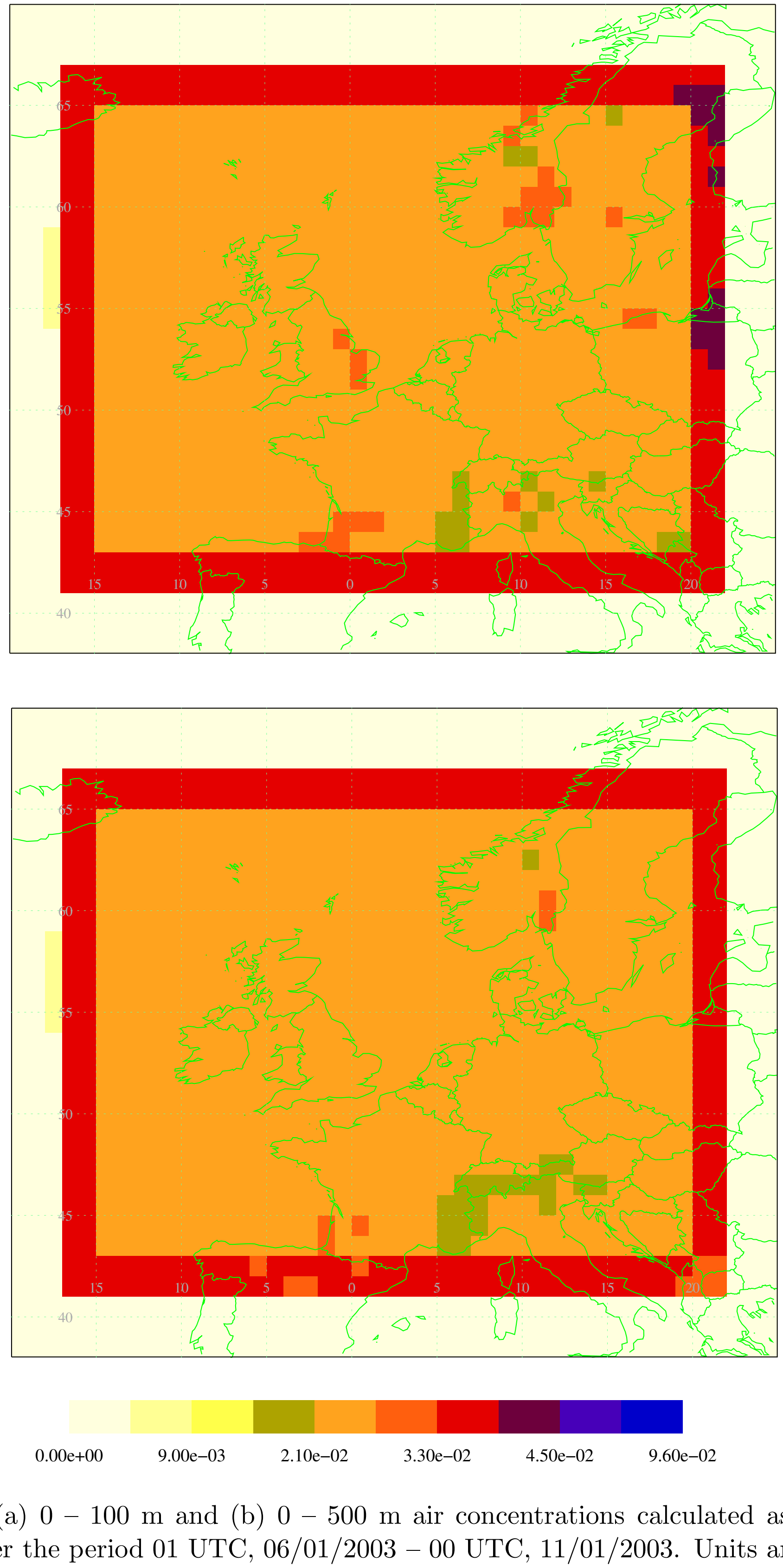

Figure 6: (a) 0 – 100 m and (b) 0 – 500 m air concentrations calculated as a 5-day average over the period 01 UTC, 06/01/2003 – 00 UTC, 11/01/2003. Units are g m^{-3}.

as for the five-day average, but at the same time there should be no obvious spatial biases in the concentration values.

Figures 7 and 8 give the hourly-average values of the $0 - 100$ m and $0 - 500$ m air concentrations, respectively, at 00 UTC for each day in the period 06/01/2003 – 11/01/2003. The results for the $0 - 500$ m air concentration are smoother than those for the $0 - 100$ m concentration because we are averaging over a greater depth of atmosphere in the former. However, apart from this difference, the features of the concentration fields are broadly similar. Deviations from the nominal concentration value are typically small: the concentration at most grid boxes is within the central band ($\pm 12.5\%$), and within a band above or below ($\pm 37.5\%$) at most of the remaining grid boxes. These deviations are largely statistical in nature (that is, random noise due to the limited number of particles) although there are some instances where the deviations have a more organised structure. For instance, deviations tend to be larger near to the Alps (with both positive and negative anomalies present); see below for a further discussion on the hourly-average time series. There is also a tendency on some occasions for elevated concentrations along the eastern coast of the UK and to the lee of the high ground of Norway (this could be a topographical effect occurring with certain wind directions, or it could be related to the wind flow near to fronts and other synoptic features). NAME III also has difficulty maintaining a uniform concentration in the vicinity of the occluded front running through Biscay and to the south west of Ireland on 08/01/2003 (third frame in the sequences). Finally, there is an extensive region of low tracer concentration over the Atlantic in the final frame, which is probably associated with the anticyclone centred over the west of the UK at this time.

Note that hourly-average values of the boundary-layer air concentration and of the vertically-integrated concentration were also calculated (but are not shown here). The boundary-layer average concentration is qualitatively similar to the $0 - 500$ m concentration. The vertical integral of concentration is generally uniform (except for the lower values expected over high orography), although synoptic-scale features can have an impact on some occasions (e.g. the small depression over Denmark on 06/01/2003 and the anticyclone over the UK on 10/01/2003 are both marked by regions with reduced total column mass of tracer). This is worthy of further exploration in the future.

Figure 9 shows time series of the hourly-average air concentration at two gridpoints in the vicinity of the Alps (the point (45.5^oN, 9.5^oE) to the south-east of the mountains, and the point (47.5^oN, 7.5^oE) to the north-west). The concentrations are calculated over the layer $0 - 100$ m, and the time series are plotted for the full duration of the model run. We observe that the time series at the north-west point is reasonably steady but that the one at the south-east point has much greater variability with some very large peaks (indeed, on one occasion, the concentration is seen to reach four times the nominal concentration value). This assessment is borne out by the respective statistics of these time series: 22.8 mg m^{-3} mean value and 3.9 mg m^{-3} standard deviation at the north-west point; and 34.8 mg m^{-3} mean value and 16.8 mg m^{-3} standard deviation at the south-east point. The target concentration is matched reasonably well, on average, at the location to the north-west of the mountains (recall that a background concentration of 24.0 mg m^{-3} is aimed for in this run). In contrast, the mean concentration at the south-east gridpoint is substantially above the target value, partly because of the very high peaks on some occasions, but there is also evidence that the concentration

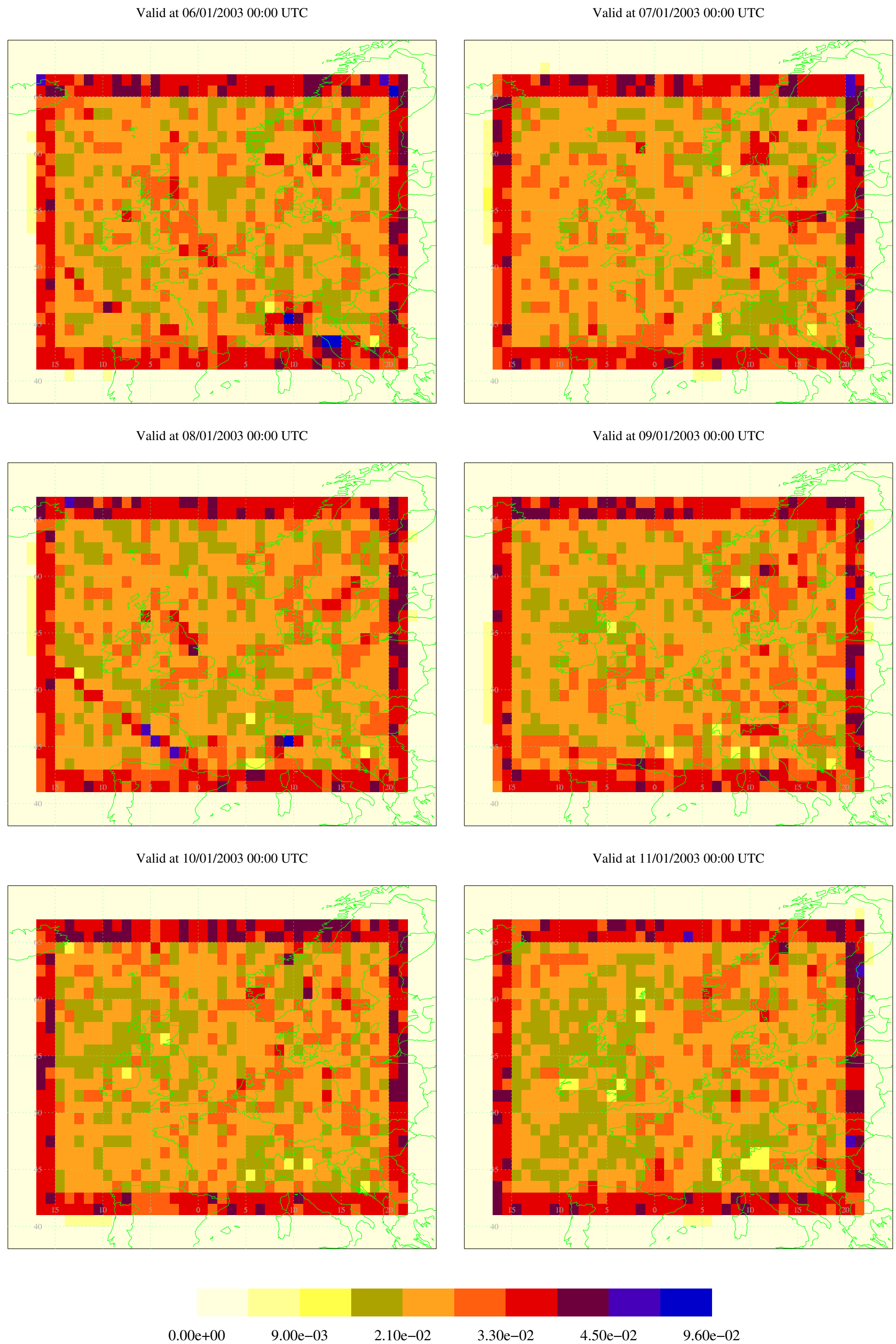

Figure 7: Hourly-average values of the 0 – 100 m air concentration shown at 00 UTC for each day in the period 06/01/2003 – 11/01/2003. Units are g m^{-3}.

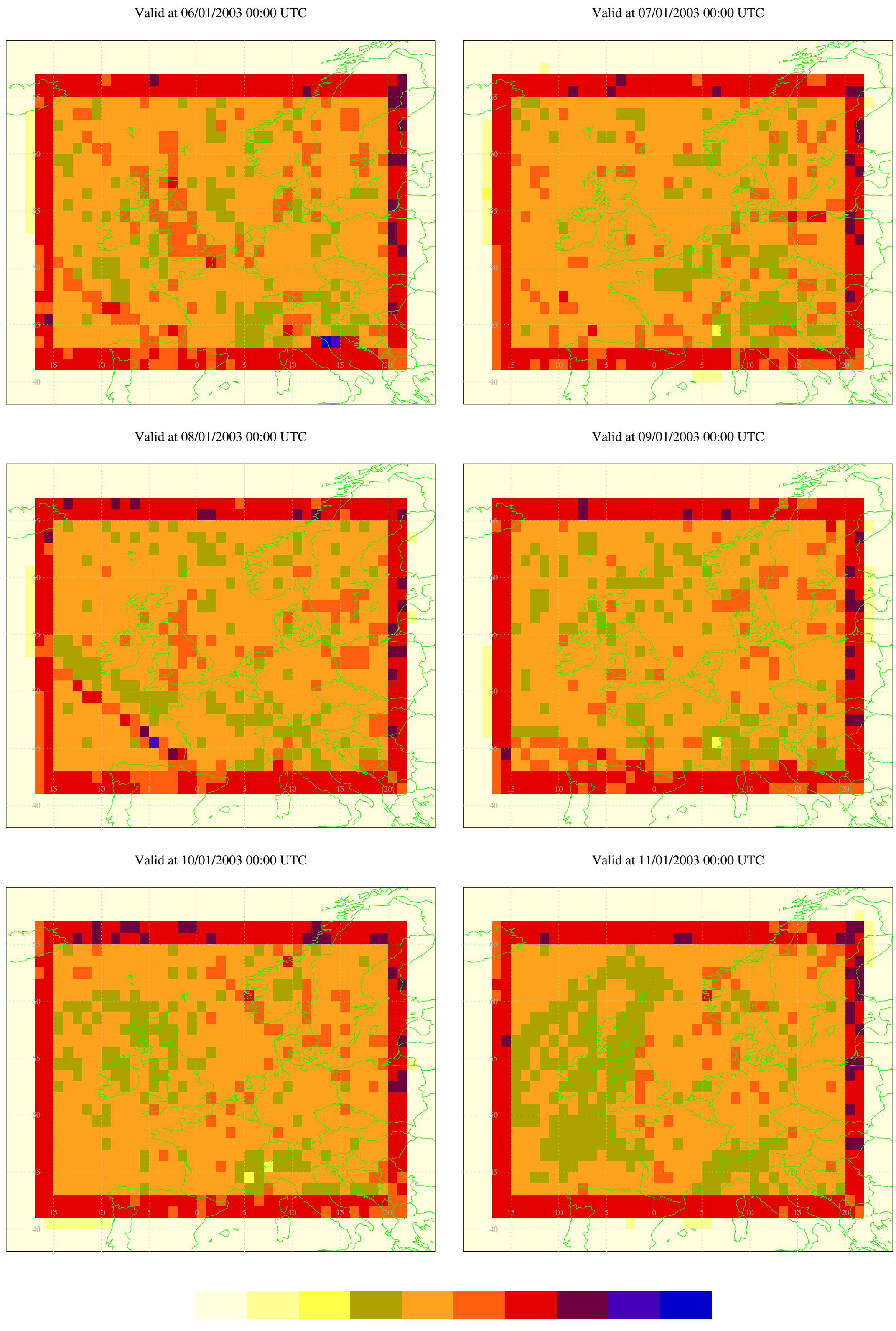

Figure 8: Hourly-average values of the 0 – 500 m air concentration shown at 00 UTC for each day in the period 06/01/2003 – 11/01/2003. Units are g m^{-3}.

is systematically too high at most other times as well (except possibly towards the end of the simulation). The variability in the time series is also much greater at the south-east point than at the north-west point (there is more than a four-fold increase in the standard deviation here). It would be worthwhile to plot hourly time series for other gridpoints around the Alpine region to get an idea of the nature and extent of the problem here. For instance, to answer the questions of whether the north-west or south-east gridpoint is more typical of time series in this region? and what role the meteorology (in particular, wind direction) plays here?

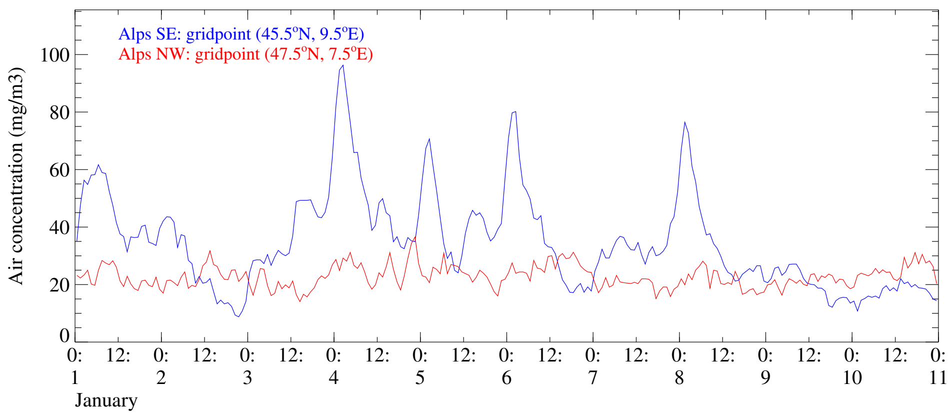

Figure 9: Time series of the hourly-average air concentration evaluated over the layer 0 – 100 m at two gridpoints in the vicinity of the Alps (one to the south-east of the mountains and the other to the north-west).

The issue of statistical noise due to the limited number of particles that are present in each grid box at any instance has been raised above. We explore this by performing an additional simulation which achieves an approximate four-fold increase in the number of particles per grid box. However, because we are limited by the total number of particles in the domain (we track approximately 2.5 million particles at any instant), the model run is restricted to a smaller primary domain covering the region (8^oW – 4^oE, 47^oN – 57^oN). Note that the target concentration is 40 mg m^{-3} in this run. Figure 10 shows hourly-average air concentration fields at 00 UTC on each of the final three days of the simulation. Here the left hand column gives concentration over the layer 0 – 100 m, and the right hand column gives concentration over the layer 0 – 500 m. Once again, it is noted that results are smoother for the 0 – 500 m output compared with the 0 – 100 m concentration, due to a greater degree of averaging obtained over the deeper layer. It is also observed that these concentration fields are smoother relative to the respective fields of the default run (c.f. the final three frames in Figures 7 and 8). This confirms that some of the variability in the earlier run is statistical in nature, but there is still a systematic component to the errors (for instance, the output at 11/01/2003 in Figure 10 indicates that there is still a tendency for elevated concentrations over eastern parts of the domain and reduced concentrations to the west at this time). It would also be interesting to repeat the 'hi-res' run with a larger modelling domain (which is now possible after recent changes to NAME III) since the reduced domain size used here might not be able to capture the full influence of large-scale features in the flow (e.g. the anticyclone over the west of the UK at the end of the simulation period).

We can further investigate the issue of statistical noise versus systematic errors (e.g. due to the meteorology) by comparing hourly time series of air concentration from several model runs. Figure 11 gives time series of hourly-average concentrations (calculated over the layer 0 – 100 m) at three locations in the UK (Birmingham, London and Narberth (SW Wales)). Three realisations (that is, model runs) are presented here. Case 1 is the standard run based on the large model domain (Figures 5 – 8). Case 2 is a second realisation (using different random numbers) but otherwise it has the same parameters as Case 1. The 'Hi-Res' Case is taken from the simulation using the reduced model domain (see Figure 10 above). Note that the time series for Cases 1 and 2 are rescaled to a target concentration of 40 mg m^{-3} to be consistent with the 'Hi-Res' Case.

Although individual time series are rather noisy here, there is clearly a systematic component to the behaviour of the time series at each location indicating that the variability is not purely statistical noise. The correlation coefficient (for Case 1 against Case 2) is roughly 0.3 at each location, supporting the claim that some variability is systematic. [We would expect zero correlation if the time series variability was purely statistical noise (as it should be), but a non-zero correlation would suggest that the origin of the deviations is more systematic and related to anomalies in the flow.] We also note that the time series in the 'Hi-Res' Case are generally less noisy (we would expect a reduction in statistical noise due to the increased number of particles).

4 Comparison with NAME II

The test case considered in this report was previously used for assessing the abilities of the NAME II dispersion model to maintain a uniform tracer field (undocumented research). Results from NAME II, v8.11 are shown here in Figure 12. As in the NAME III simulation, air concentration was calculated as an average over the last 5 days of the NAME II model simulation (i.e. over the period 01 UTC, 06/01/2003 to 00 UTC, 11/01/2003). The upper plot illustrates air concentration averaged over the vertical layer 0 – 100 m, whereas the lower plot gives concentration over the layer 100 – 500 m. The 0 – 100 m concentration is observed to be noisier than the 100 – 500 m concentration (this is due in part to the statistical sampling effect). However there also appear to be systematic problems near to the surface which are evident in the upper plot, especially the elevated concentrations over the UK, the Alps and Norway.

The plots in Figure 12 can be compared with those in Figure 6, which are equivalent results from the NAME III simulation. Note that these results cannot be compared precisely, owing to some differences in the modelling set up between the NAME II and NAME III runs. In particular, the target concentration is 40 ppb in the NAME II test (c.f. 24 mg m^{-3} mass concentration in the NAME III simulation). However the relative scaling *is* the same in each case (i.e. the central orange contour represents a range of 40 ppb $\pm$ 12.5%). Also note that the lower plot gives concentration averaged over the layer 100 – 500 m, which is different to the 0 – 500 m used in the NAME III simulations (however the impact on concentration values arising from the slight difference in vertical averaging here is likely to be small). Finally, it is not known how many particles were used in the NAME II simulation, but the noisier results suggest that it is likely to be

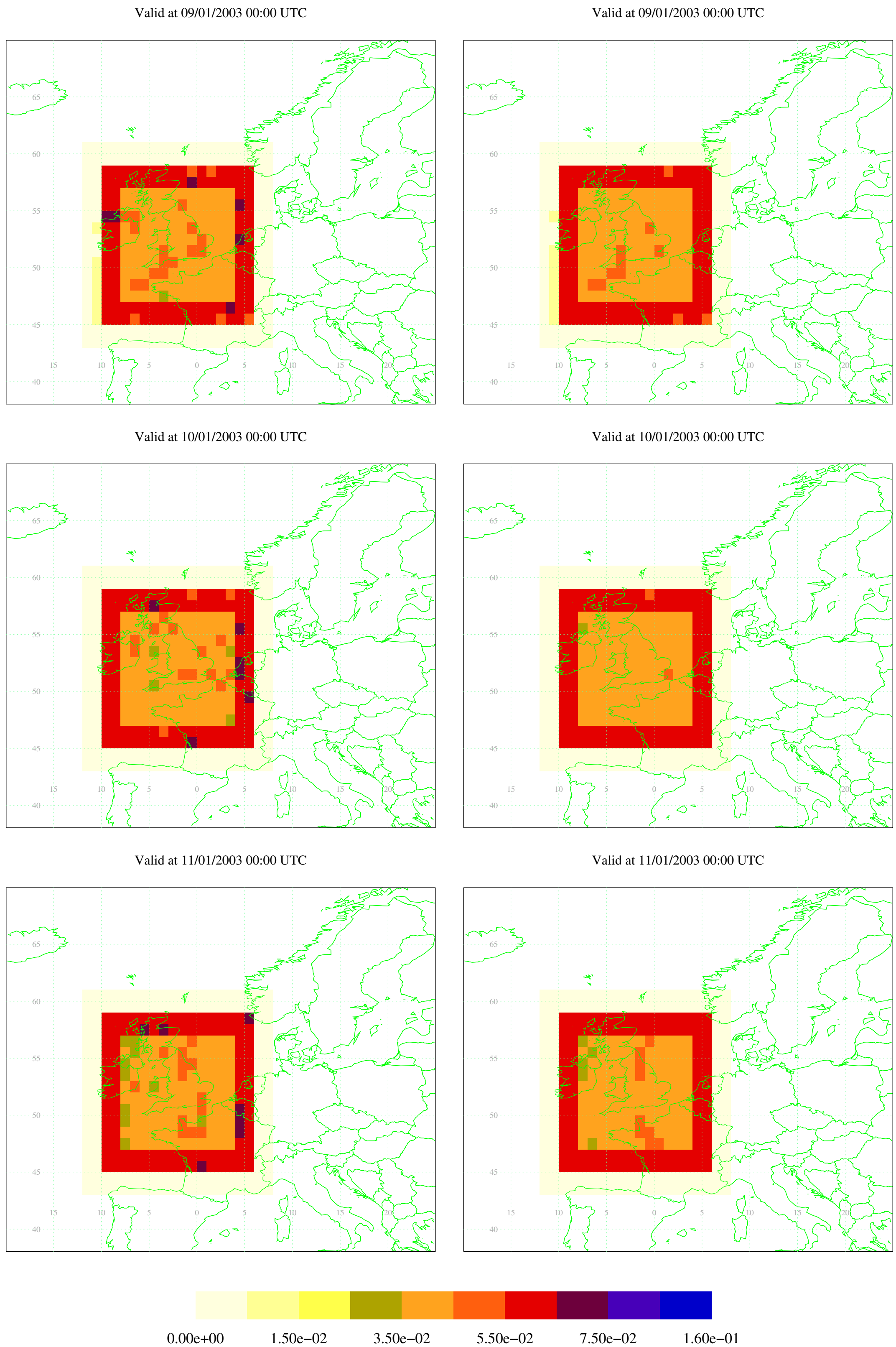

Figure 10: Hourly-average air concentrations over the layer 0 – 100 m (left column) and 0 – 500 m (right column) at 00 UTC on each of the final three days of the smaller domain run (with more particles per grid box). Units are g m^{-3}.

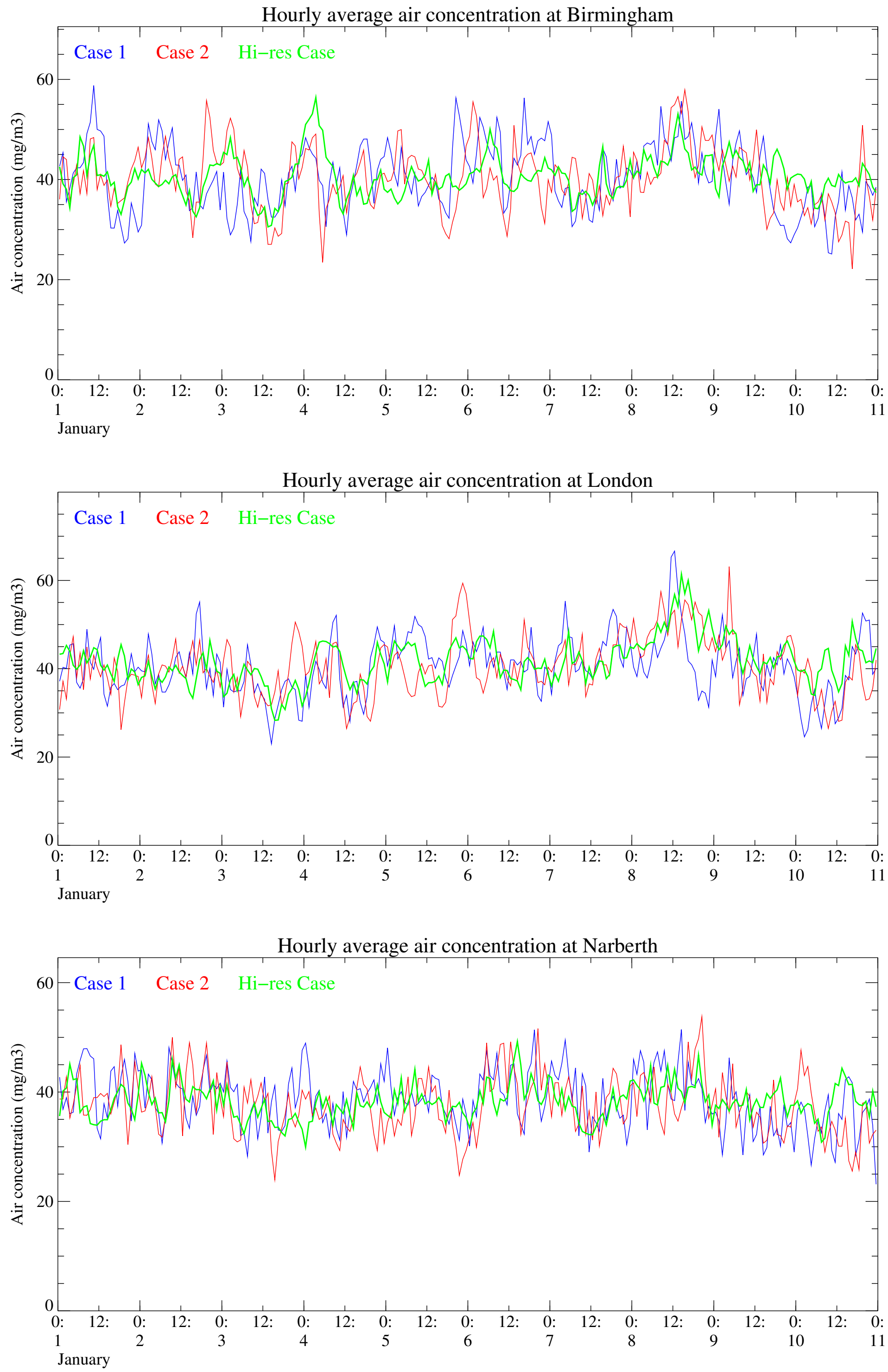

Figure 11: Time series of the hourly-average 0 – 100 m air concentrations at three locations in the UK (Birmingham, London and Narberth). Three realisations are shown: two standard runs (Cases 1 and 2) use the default (i.e. large) model domain; and a 'Hi-Res' Case uses a reduced domain to allow a greater number of particles per grid box.

fewer than in the NAME III run.

The NAME III predictions are a significant improvement on those of NAME II. This may be partly related to a reduction in statistical noise arising from modelling a greater number of particles in the NAME III simulations, but there are also clear systematic improvements (for instance, over the UK, where the elevated concentrations near to the ground are largely absent in the NAME III results). The improvements are likely to be attributable to a variety of model differences, but one significant influence is the different handling of NWP met data in the two models. NAME II interpolates all meteorological parameters onto a single met grid, whereas NAME III can handle parameters on their native (staggered) grids. This will have an effect on mass conservation of the flow field, and probably explains some of the improvements seen in the NAME III results.

5 Concluding remarks

The report discusses the ability of NAME III to maintain a uniform tracer concentration within the modelling domain when forced by a uniform concentration around the edges. Such a characteristic is desirable because it implies that material is transported in a conservative manner – this can be especially significant in some dispersion applications such as modelling of long-range transports and slow chemistry processes. The results presented here demonstrate that NAME III performs reasonably well in this test case, although difficulties are sometimes experienced, especially in areas with steep orography such as the Alps. Comparison with an earlier test of NAME II suggests that NAME III provides a significant improvement over its predecessor in this particular case. This improvement is likely to be, at least in part, a consequence of NAME III using NWP met fields on their native staggered grids (rather than the interpolation to a single grid performed in NAME II). It is quite probable that this interpolation previously degraded mass conservation in the dispersion modelling.

Some final comments and suggestions for further investigation are noted below. Firstly, more recent versions of NAME III are able to handle more particles (at least, for 'cheap' particle applications such as the uniform field test considered here). This should permit any future tests to consider a greater number of particles and so reduce the impact of statitical noise on results. It would be beneficial in future simulations to request time series output at more locations, especially in problem areas such as around the Alps, for instance. Statistics of the time series and fields output would also be useful (e.g. standard deviations of concentration). Standardising the target concentration (say at 1 g m^{-3}) might aid future analysis of results.

The analysis presented here is based on a single test case over one time period. It would be informative to repeat the modelling exercise for other dates to sample different meteorological situations. Similarly, this single test case only considers UM 5 meteorology (regional data), but it would be useful to assess the performance of NAME III with other sources of met data (e.g. with UM 4 meteorology or ECMWF data). Finally, a closer study of the meteorology in problem areas could provide some guidance on the nature of these difficulties (e.g. how do problems near the Alps vary with wind direction, etc.; issues near to frontal boundaries).

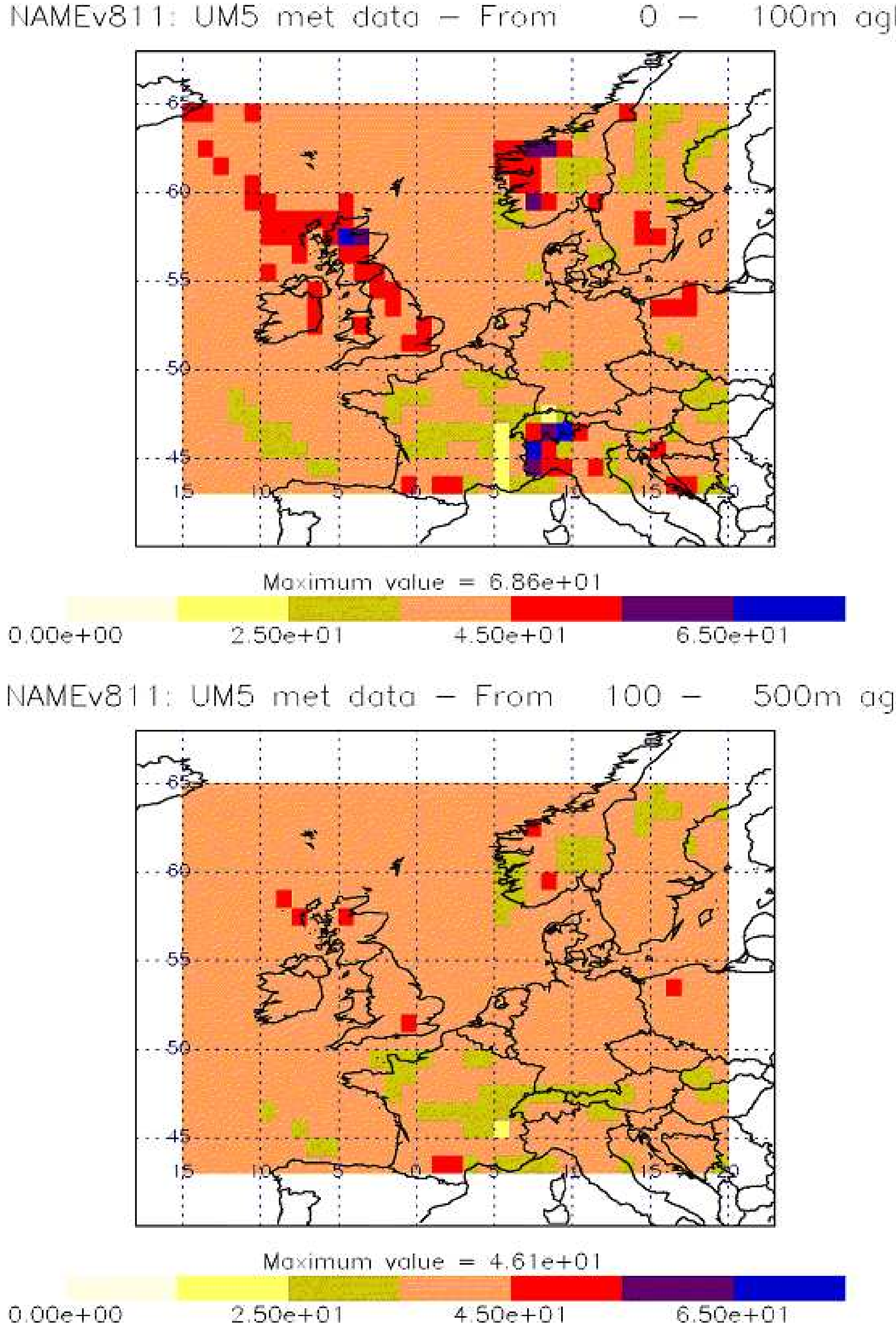

Figure 12: (a) 0 – 100 m and (b) 100 – 500 m air concentrations from NAME II (v8.11), calculated as a 5-day average over the period 01 UTC, 06/01/2003 – 00 UTC, 11/01/2003. Units are ppb, and the target concentration is 40 ppb in this test.

Appendix A: Analysis charts for 01/01/2003 – 11/01/2003

00 UTC, 01/01/2003

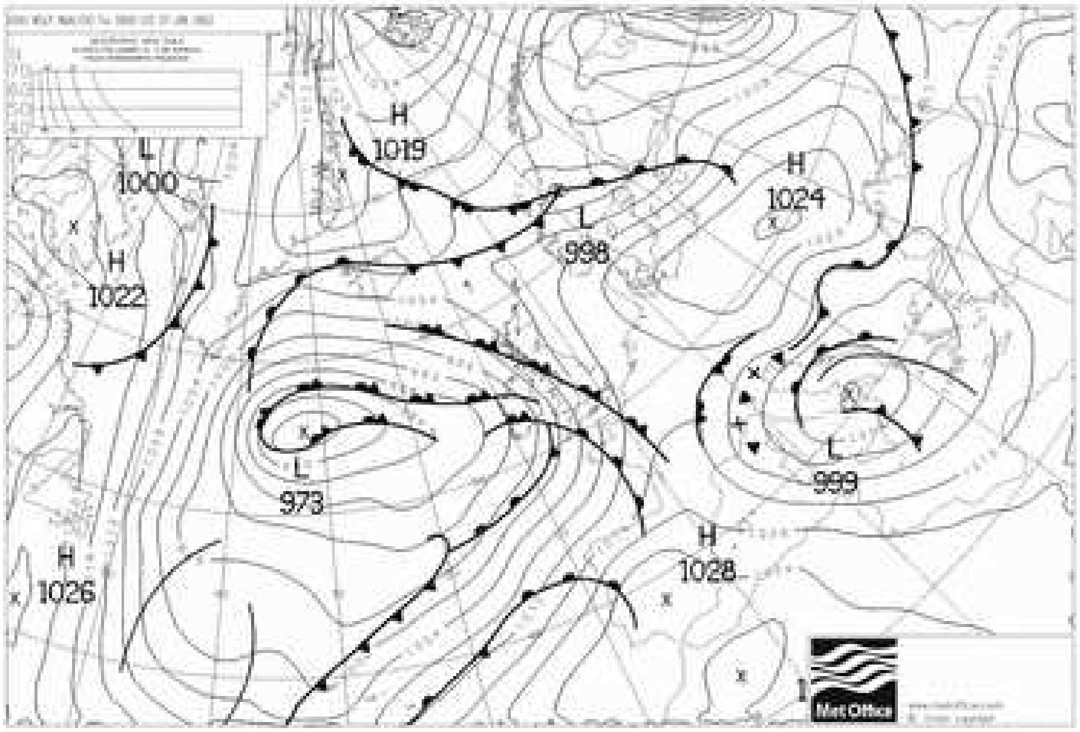

00 UTC, 02/01/2003

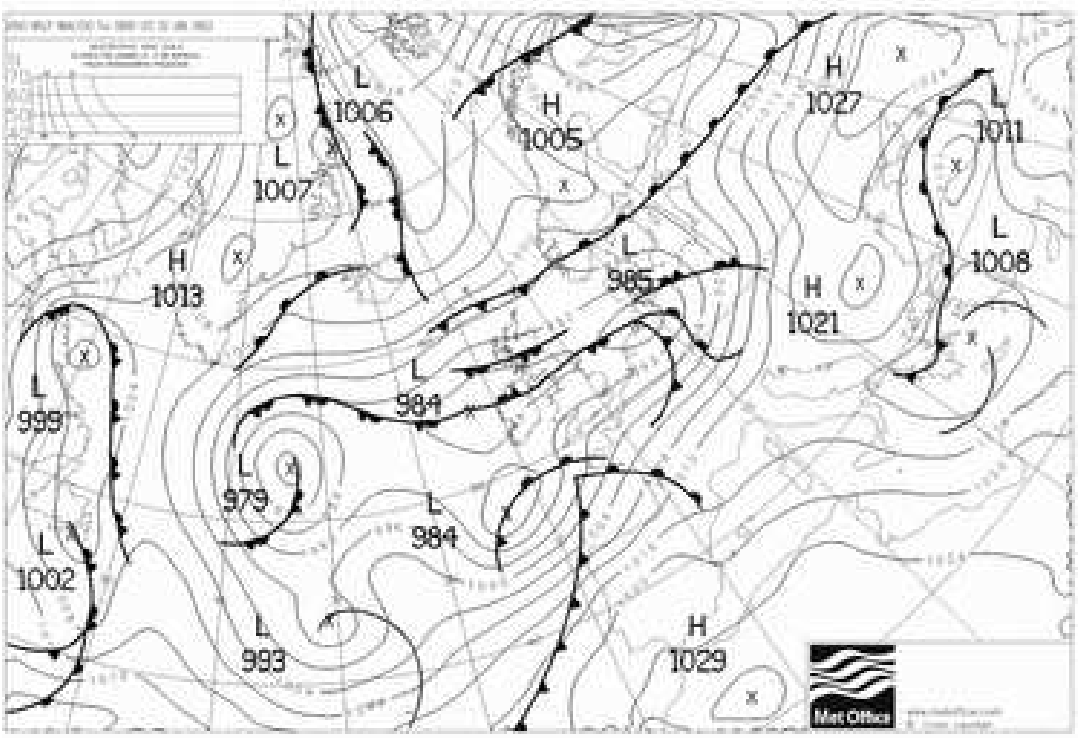

00 UTC, 03/01/2003

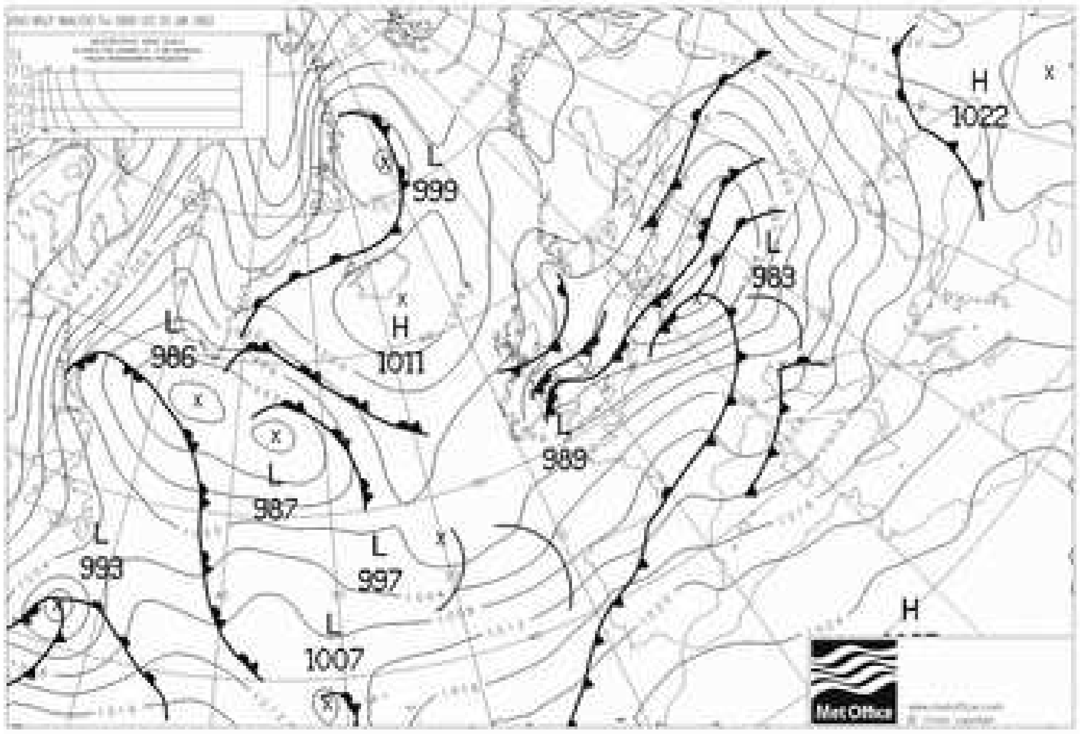

00 UTC, 04/01/2003

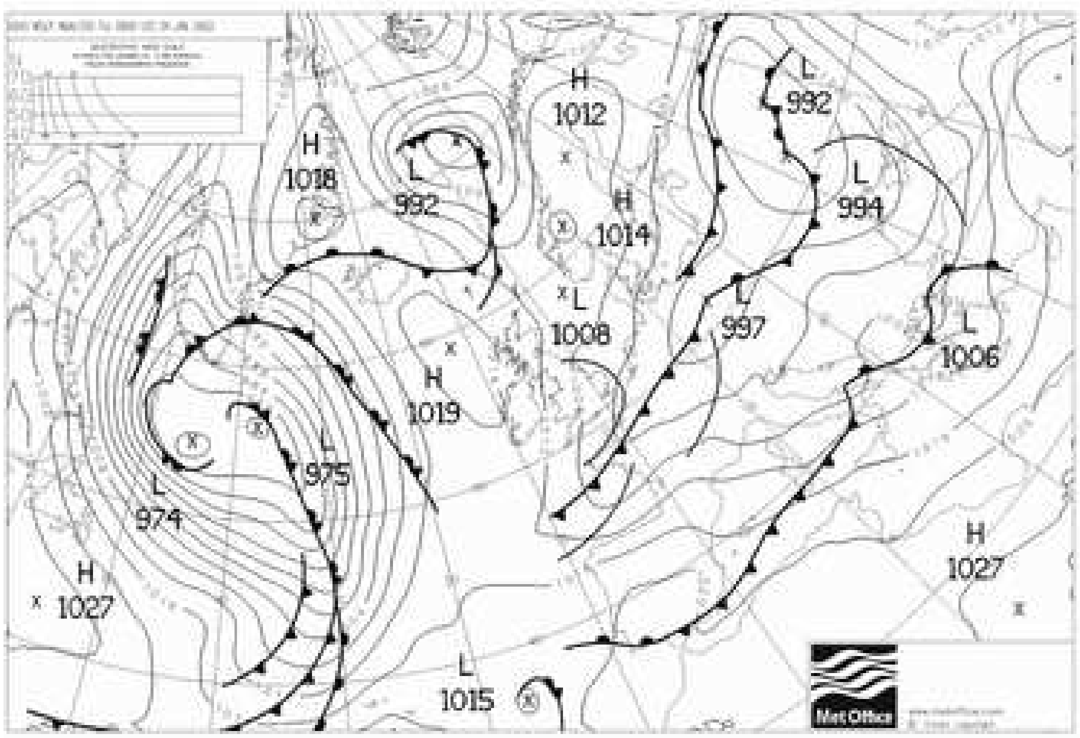

00 UTC, 05/01/2003

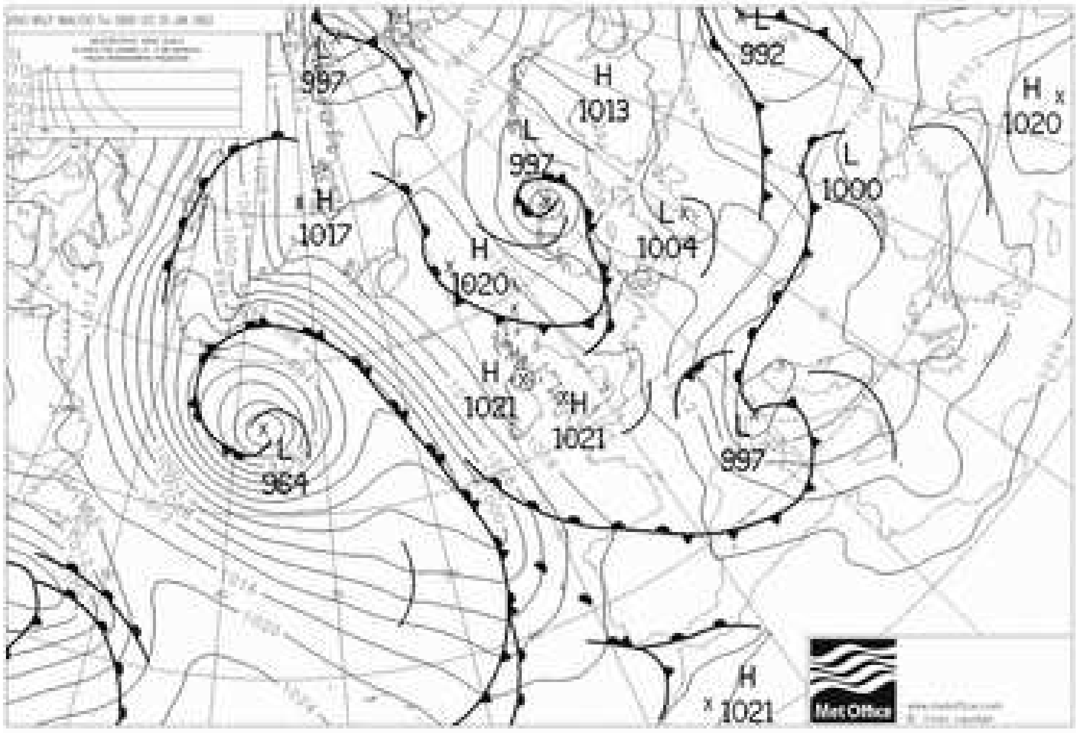

00 UTC, 06/01/2003

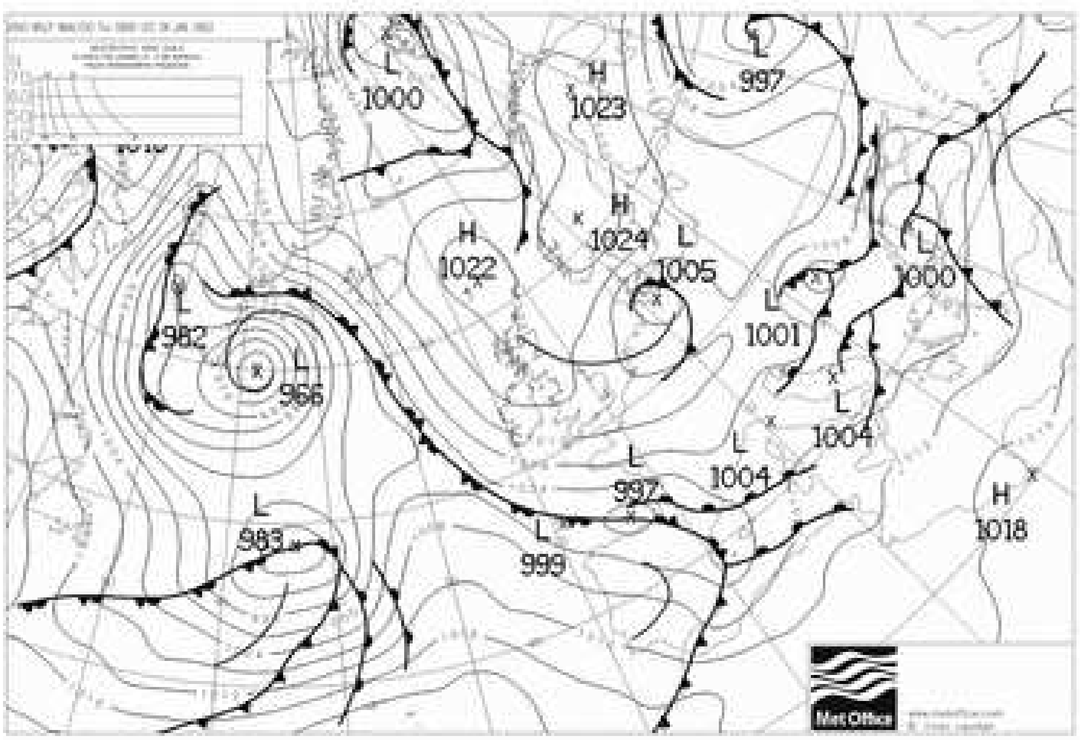

00 UTC, 07/01/2003

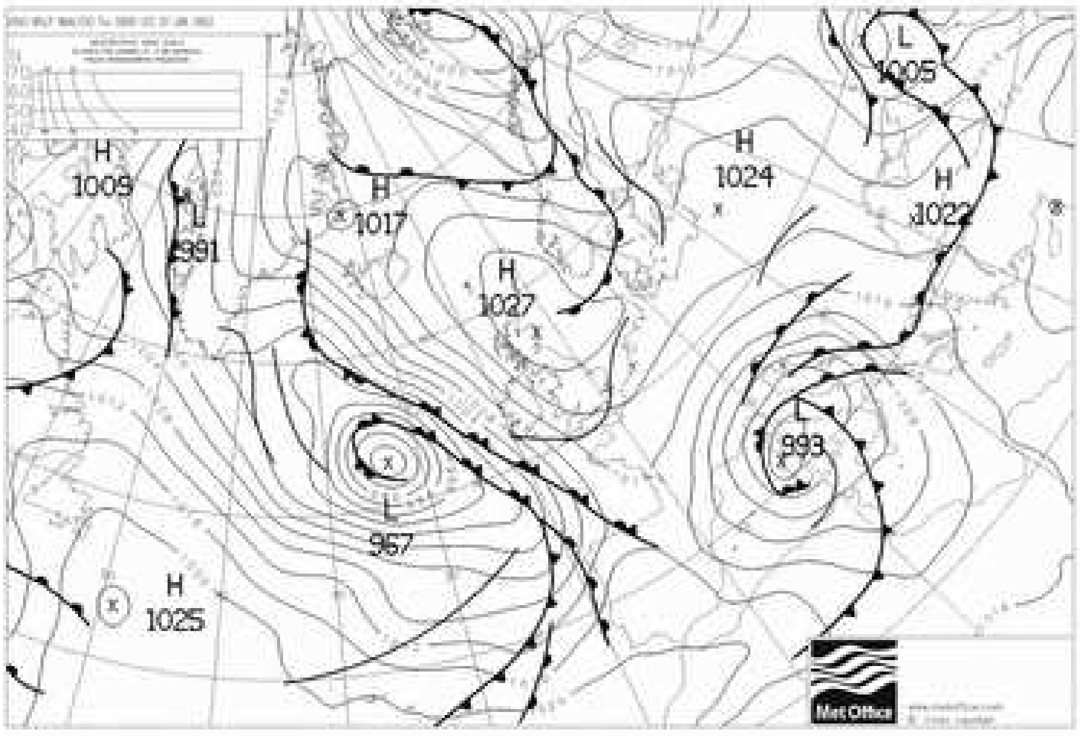

00 UTC, 08/01/2003

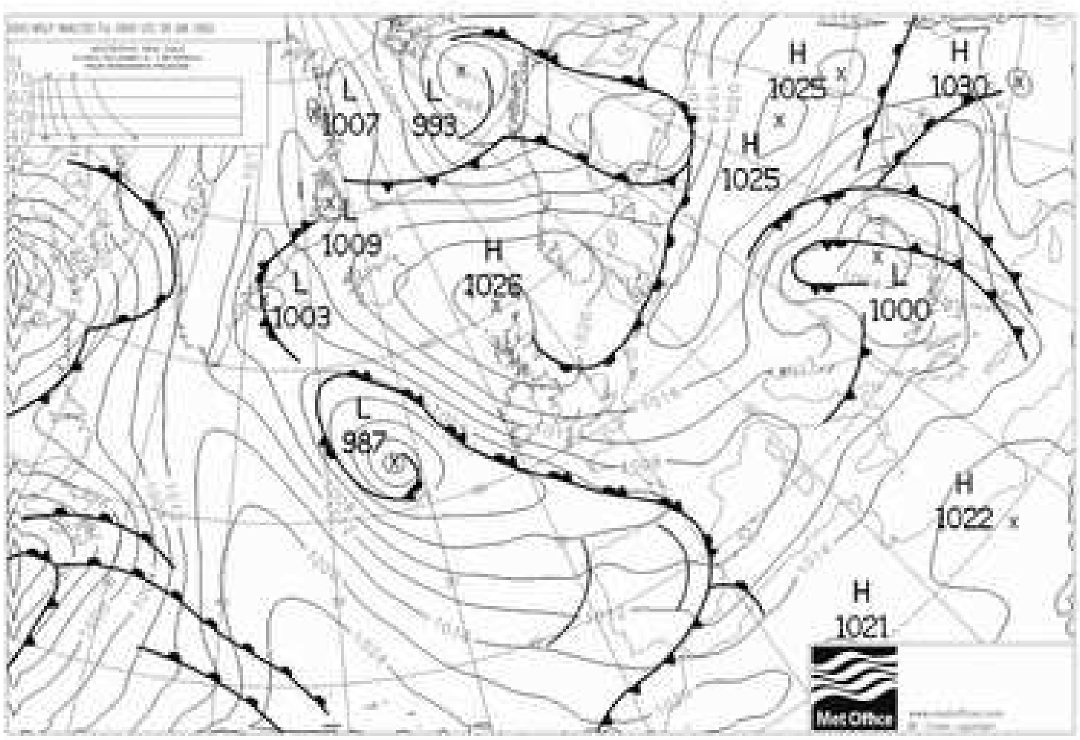

00 UTC, 09/01/2003

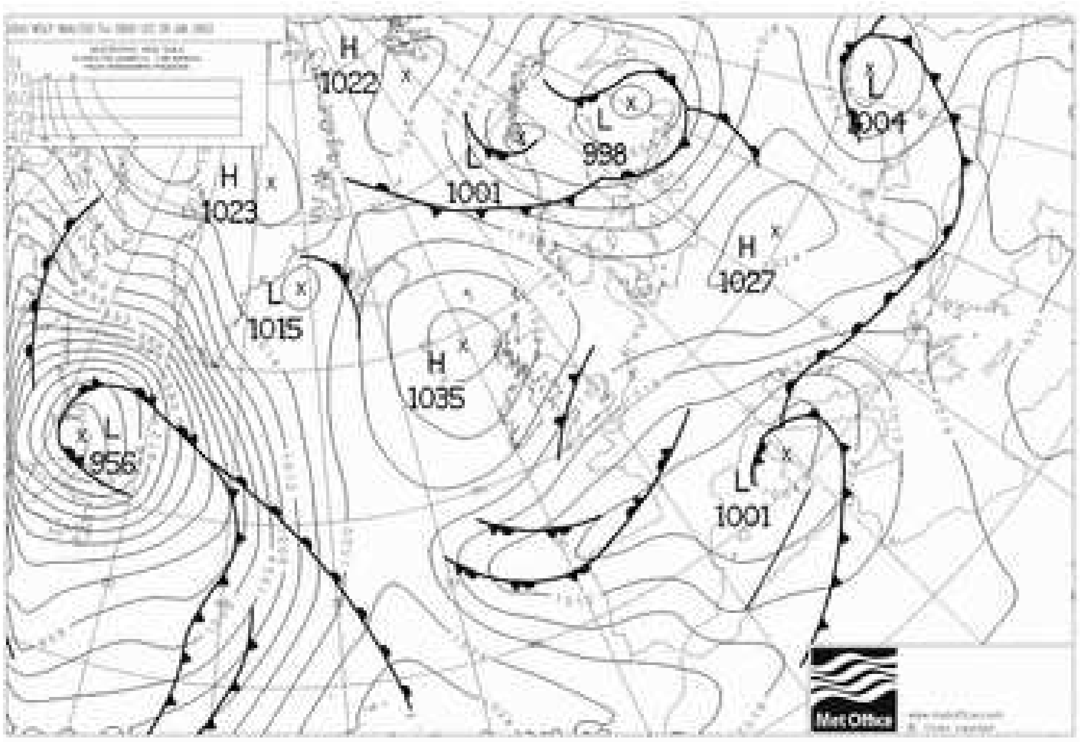

00 UTC, 10/01/2003

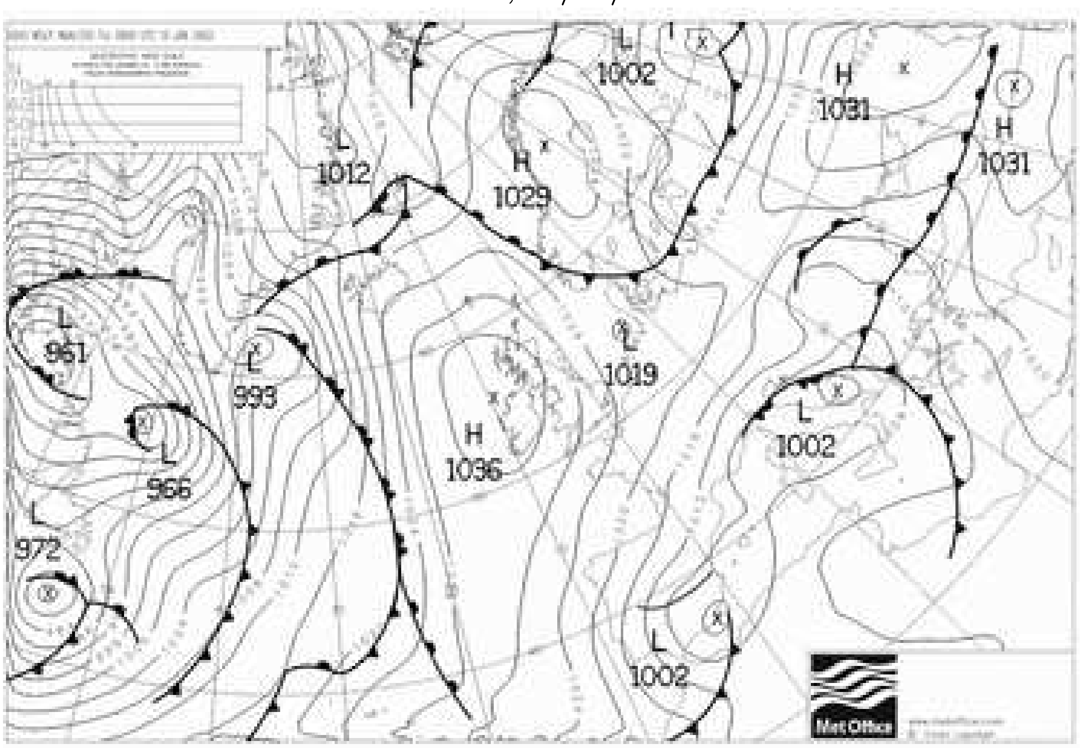

00 UTC, 11/01/2003